Original Research Article

Diffusion Weighted MR and Dynamic Contrast Enhanced MRI for Characterization of Ovarian Tumors

Abstract

Background:

For comprehensive internal architecture identification of ovarian tumors, DCE-MRI is advised. An imaging technique known as diffusion weighted (DW) assists in differentiating between benign and malignant lesions. The purpose of this study was to assess the effectiveness of DCE-MRI and diffusion-weighted MRI in characterizing ovarian cancers and distinguishing malignant from benign tumors.

Methods: This retrospective study was carried out on 40 patients aged from 21 to 63 years old presented by ovarian masses based on clinical examinations and on US study.All patients were subjected tofull history taking, laboratory investigations including pregnancy tests, complete blood counts and some tumour markers, pelvi-abdominal ultrasound and MRI.

Results: MRI have a sensitivity of 53.85 %, a specificity of 92.59 %, positive predictive value (PPV) of 77.78 %, negative predictive value (NPV) of 80.65 % and accuracy of 80% compared to pathology of the studied patient. DCE has a sensitivity of 67.15 %, a specificity of 100%, PPV of 100%, NPV of 79.4% and accuracy of 82.5%. compared to pathology of the studied patient. DWI score at a cut-off point (≤1.1) predicted patients with malignant ovarian tumours, with 97% accuracy, sensitivity of 88.89% and specificity of 100% ($p < 0.001$). There was a high statistical significance between findings on DWI-MRI, DCE-MRI, and pathological types ($P < 0.001$ for benign versus malignant lesions). Higher magnetic

resonance elastography (MRE) was seen with malignant ovarian lesions (MRE < 85% suspected malignancy).

Conclusions: Conventional MR images are the mainstays for assessment of patients with adnexal lesions. The addition of DWI and DCE-MR imaging enhances the specificity of MRI, boosting the radiologist's confidence in picture interpretation and ultimately affecting the patients' prognosis.

Keywords: Diffusion weighted MR, Dynamic contrast enhanced MRI, Ovarian Tumors.

Introduction:

The second most frequent gynecologicaltumors and the fifth most prevalent tumors in women are ovarian tumors. The preoperative assessment of complicated adnexal masses is essential for determining the potential surgical methods since these tumors are the main reason for gynecologic operations [1].

The initial imaging method for adnexal lesions is ultrasonography (US), which is also helpful for classifying non-complex lesions. Malignant tumors may be accurately characterized by magnetic resonance imaging (MRI), especially when US results are uncertain or unsatisfactory [2-4].

In the examination of cancer patients for initial assessment and the evaluation of therapeutic response, functional imaging is playing a bigger role. Recent technological developments enable the utilization of dynamic and diffusion MRI in applications for the abdomen and pelvis [5].

On T1- and T2-weighted scans, MRI may show morphologic features as papillary projections, septations, nodularity, solid components, and signal intensity, however none of these can properly differentiate between malignant and benign lesions [6, 7].

Dynamic contrast-enhanced magnetic resonance imaging (DCE-MRI) relies on the contrast material leaking into extracellular space from capillary walls to provide quantitative data that represents blood flow and vascular permeability [8].For comprehensive internal architecture identification of ovarian tumors, DCE-MRI is advised, particularly for delineating necrosis, solid components, papillary projections, peritoneal implants, and septations [9].

Recent studies assessed the effectiveness of DCE-MRI for additional adnexal mass characterization. It offers details on the vascularity and perfusion of the tumor as well as other post-processing quantitative information [10].

An imaging technique known as diffusion weighted (DW) assists in differentiating between benign and malignant lesions by providing quantitative measurements of apparent diffusion coefficient (ADC) values. These measurements provide information about the cellular proliferation of the tissue and can be used to reveal viable tumors apart from treatment-related developments [11].

The translational motion of water molecules is also related to ADC. Increased tumor cellularity, which attempts to limit water transport, is correlated with lower ADC levels. It may be employed as a predictor for therapeutic response and in the assessment of recurrence and multi focality since increasing ADC values are seen in carcinomas responding to radiotherapy [12-14].

The purpose of this study was to assess the effectiveness of DCE-MRI and diffusion-weighted MRI (DW-MRI) in characterizing ovarian cancers and distinguishing malignant from benign tumors.

Patients and Methods:

This retrospective study was carried outon 40 patients aged from 21 to 63 years old presented by ovarian masses based on clinical examinations and on US study who were referred from Oncology Department and outpatients clinic to the Radiodiagnosis Department Faculty of Medicine, Tanta University hospital.

After receiving authorization from Tanta University Hospitals' Ethical Committee, the research was carried out. The patients provided signed permission after being fully briefed.

Exclusion criteria were metallic prosthesis, cardiac pacemakers, insulin pumps, neuro-stimulators, cochlear implants, history of claustrophobia or presence of renal impairment.

Every patient has undergone a thorough history taking process with a focus on the following factors: age, parity, menstrual history, and previous gynaecological issues or surgeries, laboratory investigations including pregnancy tests, complete blood counts and some tumour markers, pelvi-abdominal US and MRI.

MR imaging protocol

Non contrast study: Axial T1-weighted imaging with a TR/TE of 500/10 milliseconds and axial T2-weighted scans with a TR/TE of 3300/100 milliseconds, slice thickness of 6 mm, gap of 1 mm, FOV of 32-42 cm, and matrix of 256 × 256. Sagittal and coronal T2-weighted scans with a slice thickness of 8 to 10 millimeters, a gap of 1 millimeter, a matrix of 256 × 256 and a FOV of 40 to 50 centimeterswere obtained.

DW-MRI: Prior to the injection of contrast media, DW-MRI was obtained in the axial plane, having b values (0, 300, and 600). TR/TE, 5000/70 with a slice thickness of 6 mm, a gap of 1 mm, a FOV that ranges from 36-40 cm, and a matrix that is 128 × 128.

MRI with dynamic contrast enhancement: Following manually administering gadolinium at a dosage of 0.1 mmol/kg of body weight (20 ml maximally), post-contrast T1 fat-sat

imagingwere acquired directly after the procedure. Images were taken in intervals of 0, 30, 60, 90, and 120 seconds.

The following was determined from an analysis of MR images: Magnitude of the lesion, solid component enhancement if existent, tumor signal intensity, existence of septations and vegetations, distribution and size of their enhancement, wall thickness and uniformity of the tumor, and MR morphology of the tumor—whether solid, cystic, or mixed. The existence of ascites, the existence of peritoneal deposition, and the invasion of other pelvic organs were also examined in MR images.

Simple cystic tumors have increased signal intensity on T2-weighted scans without a solid component but low signal intensity on T1-weighted imaging. Complex benign-looking masses: T1WI high signal intensity is interpreted as either blood or fat. Low signal is shown on fat-suppressed pictures, whereas blood still shows a strong signal.

As according Kishimoto et al. [15], the appearance of wall thickness greater than 3 mm and solid vegetation greater than 1 cm qualified as malignant MR criteria. The presence of necrosis and patches of thick septa >3 mm. Regarding staging, swollen lymph nodes, ascites, and peritoneal deposit are indications of tumor dissemination. Using post-contrast pictures, it was possible to identify enhancements in the solid component, tumor wall, septations, and vegetations.

Interpretation of DWI

Qualitative analysis: In terms of signal intensity, benign masses had low signal on DWI and high signal in the accompanying ADC maps (facilitated diffusion), while malignant masses had high signal on DWI and low signal in the accompanying ADC maps (limited diffusion).

Quantitative analysis: ADC map was created for the quantitative analysis of DWI, and the solid and cystic tumor components were chosen as the ROI (region of interest), which was then automatically computed on the computer to generate the ADC values.

Interpretation of DCE-MRI

Consensus analysis of dynamic data was performed at a workstation. The five-point dynamic run capture at 0-, 30-, 60-, 90-, and 120-seconds following gadolinium administration includes the whole mass. A curve of signal intensity (SI) and time was created. There were three different sorts of curves: Type I exhibited a gradual ascent without a clear peak, Type II a modest initial enhancement followed by a plateau, and Type III a fast steep beginning enhancement and quick washout. The computer program automatically determined the maximum relative enhancement (MRE), and malignancy was detected with greater than 85%.

Statistical analysis

The SPSS v15 statistical analysis programwas used. When applicable, frequency and percentages, median and range, or mean and standard deviation (SD) were used to statistically characterize the data. The student's t test for independent samples was used to compare numeric values between the research groups. Exact or Chi square tests were used to compare categorical data. Sensitivity, specificity, positive and negative predictive values, and total accuracy were used to describe accuracy. Additionally, the unpaired t test and McNemar test were used to compare the groups. The Pearson correlation was used to look for correlations. It was deemed statistically significant if $p < 0.05$.

Results:

In comparison to the benign group, the malignant group's age and CA 125 plasma level were considerably higher (P value <0.001). Between the two groups, there was no significant disparity in the lateralization of the lesion (P value >0.05). Table 1

Table1: Comparison between benign and malignant groups regarding age, laterality of lesion and CA 125 serum level of the studied patient

		Benign group (n= 26)	Malignant group (n= 14)	P-value
Age(years)		33.64±9.3	46.58± 11.12	<0.001*
Side	**Bilateral**	7 (26.9 %)	5 (35.7 %)	0.84
	Left	11 (42.3 %)	5 (35.7 %)	
	Right	8 (30.8 %)	4 (28.6 %)	

CA 125 serum level (U/ml)	28±20	380.35±400.23	<0.001*

Data are presented as mean ± SD or frequency (%), * significant as P value ≤ 0.05. CA: Cancer antigen.

Table 2 shows the dimensions of benign and malignant lesions, composition and signal intensity (SI) of ovarian lesions of the studied patients.

Table 2: The dimensions of benign and malignant lesions, composition and signal intensity (SI) of ovarian lesions of the studied patients

Dimensions		**Benign lesions**	**Malignant lesions**
Minimum		1.5 cm	3.5cm
Maximum		30 cm	24cm
Composition of the lesions			
Cystic	**Complex**	20 (50 %)	
	Pure	8 (50 %)	
	Mixed	7 (17.5 %)	
Solid		5 (12.5 %)	
SI on T1 WI			
High		7 (17.5 %)	
Low		18 (45 %)	
Mixed		15 (37.5 %)	
SI on T2 WI			
High		18 (45 %)	
Low		7 (17.5 %)	
Mixed		15 (37.5 %)	

Data are presented as frequency (%), SI: Signal intensity.

Table 3 showtypes of ovarian masses recognized by conventional MRI and MRI O-RADS score of the studied patients. In the benign group, 17/26 cases showed O-RADS MRI score 2, and 9/26 cases scored 3. None of the benign cases showed O-RADS MRI score 4 or 5. Six of the malignant cases scored 4 on the O-RADS score and 8 cases scored 5. The optimal cut-off value for predicting malignancy was >O-RADS 3

Table 3: Types of ovarian masses recognized by conventional MRI and MRI O-RADS score of the studied patients

Conv. MRI mass		
Benign		25 (62.5 %)
Malignant		9 (22.5 %)
Borderline	**Suspected malignant (5)**	6 (15 %)
	Suspected benign (1)	
ORADS MRI score		
2		17 (42.5 %)
3		9 (22.5 %)
4		6 (15 %)
5		8 (20 %)

Data are presented as frequency (%), MRI: Magnetic resonance imaging, ORADS: Ovarian-adnexal reporting and data System.

MRI have a sensitivity of 53.85 %, a specificity of 92.59 %, PPV of 77.78 %, NPV of 80.65 % and accuracy of 80% compared to pathology of the studied patient. DCE has a sensitivity of 67.15 %, a specificity of 100%, PPV of 100%, NPV of 79.4% and accuracy of 82.5%. compared to pathology of the studied patient. DWI score at a cut-off point (≤1.1) predicted patients with malignant ovarian tumours, with high (97%) accuracy, sensitivity of 88.89% and specificity of 100% ($p < 0.001$).

Table 4: Results of conventional MRI, DCE compared to pathology of the studied patient and DWI as a predictor in prediction of malignant ovarian tumors in the studied patients

	Sensitivity	Specificity	PPV	NPV	Accuracy
Conventional MRI	53.85 %	92.59 %	77.78 %	80.65 %	80%
DCE	67.15 %	100%	100%	79.4%	82.5%
DWI					
Cutoff value	**Sensitivity**	**Specificity**	**Accuracy**	**AUC**	**p-value**
<1.1	88.89 %	100%	97%	0.995	<0.001*

* Significant as P value ≤ 0.05. DWI: Diffusion-weighted imaging, DCE: Dynamic contrast-enhanced, MRI: Magnetic resonance imaging.

There was a high statistical significance between findings on DWI-MRI, DCE-MRI, and pathological types (P values <0.001 for benign versus malignant lesions). Higher MRE was seen with malignant ovarian lesions (MRE more than 85% suspected malignancy). Time of peak was insignificantly different between both groups. Table 5

Table 5: Comparison between benign and malignant groups regarding DWI-MRI, DCE-MRI, time of peak values, MRE values of the studied patients

		Benign group (n= 26)	Malignant group (n= 14)	P-value
DWI-MRI		1.84±0.8	1.1± 0.42	<0.001*
DCE-MRI	**Type I**	26 (100 %)	0 (0 %)	<0.001*
	Type II	0 (0 %)	8 (57.2 %)	
	Type III	0 (0 %)	6 (35.7 %)	
Time of peak		102.4 ± 55.52	78.3 ± 21.94	0.23
MRE		84.7 ± 28.93	220.9 ± 62.18	0.001*

Data are presented as mean ± SD or frequency (%), * significant as P value ≤ 0.05. DWI-MRI: Diffusion-weighted imaging magnetic resonance imaging, DCE-MRI: Dynamic contrast-enhanced MRI, MRE: Magnetic resonance elastography.

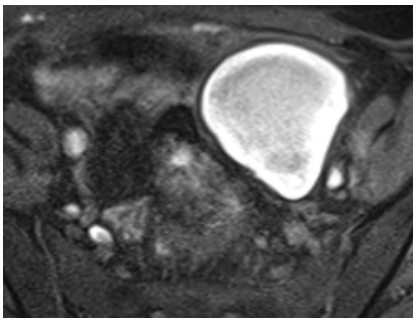

(a) Axial T1 WI

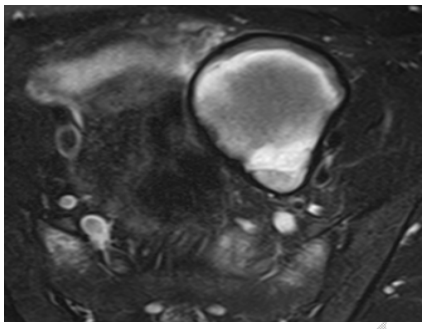

(b) Axial T2WI.

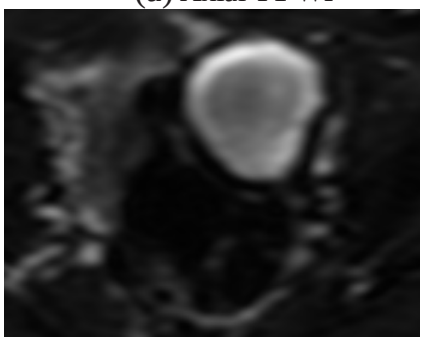

(c) DWI

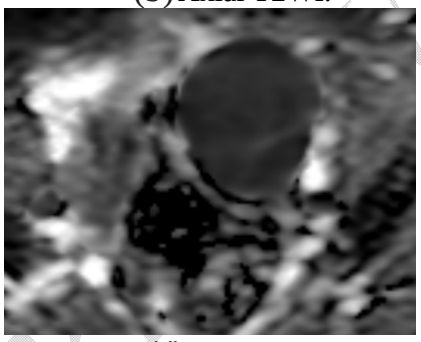

(d) ADC map

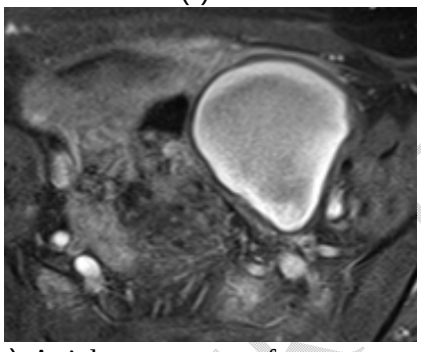

(e) Axial post contrast fat suppressed T1

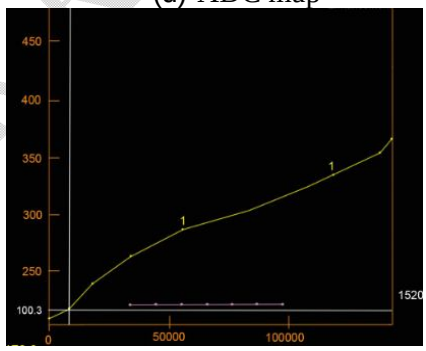

(f) Post processing time intensity curve;

Figure 1: shows a left ovarian unilocular cystic lesion, measuring about 6.5x5.5cm in dimensions, with relatively thickened wall, eliciting high signals on T1WI (a), intermediate to high signals with hemosiderin deposition on T2WI(b), restricted diffusion (c), ADC value of ($0.78x10^{-3}$ mm2 /s) (d), mild wall enhancement (e) and type 1 time intensity curve (slow rising), denoting its benign nature (f)

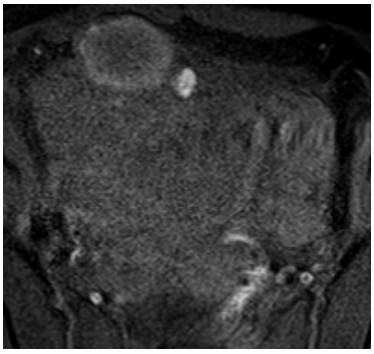

(a) Axial T1 WI

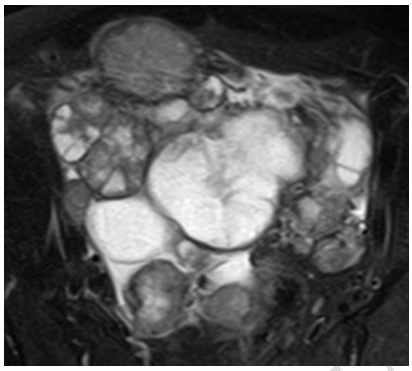

(b) Axial T2 WI

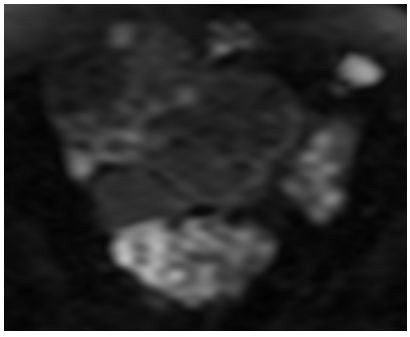

(c) DWI

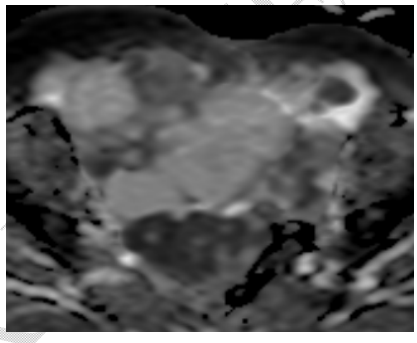

(d) ADC map

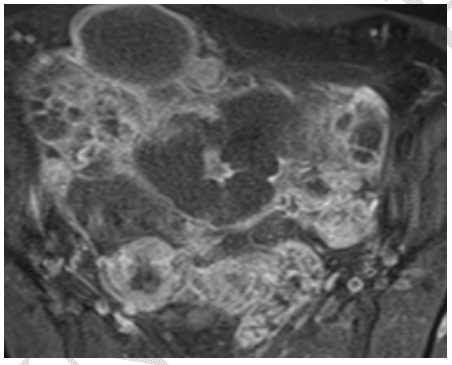

(e) Axial post contrast fat suppressed T1

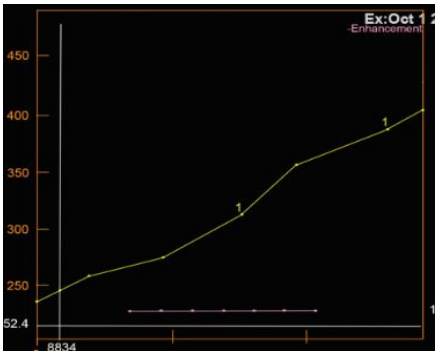

(f) Post processing time intensity curve

Figure 2: shows bilateral large dominantly cystic adnexal lesions ,measuring about 9x8cm on the right side and 7.5x4.5cm on the left side with thick septations and solid components , eliciting predominantly low signals with small areas of high signals on T1WI(a), predominantly high signals on T2WI(b) , restricted diffusion of the solid components and facilitated diffusion of the cystic components(c), ADC value of ($1.2x10^{-3}$ mm2/s) (d), moderate wall and septal enhancement (e) and type I time intensity curve (slow rising curve), suggesting its benign nature (f)

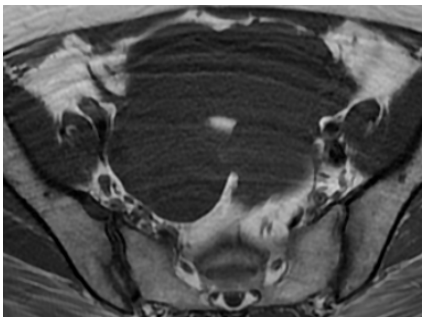

(a)Axial T1WI

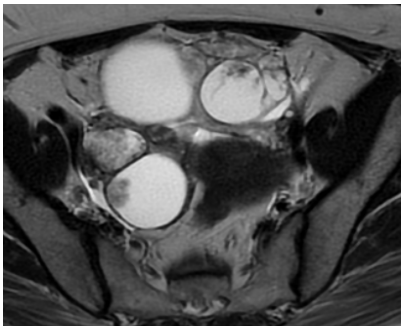

(b) Axial T2WI

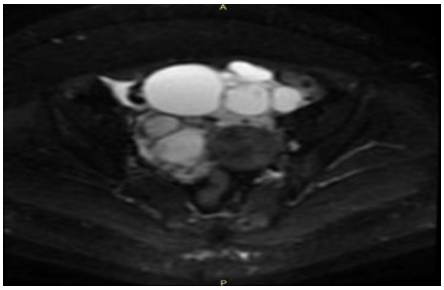

(c) DWI

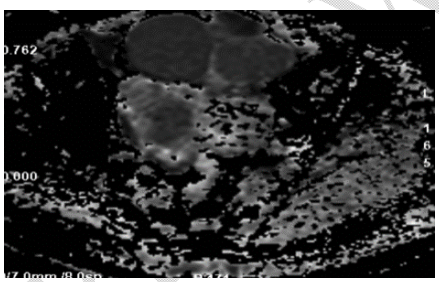

(d) ADC map

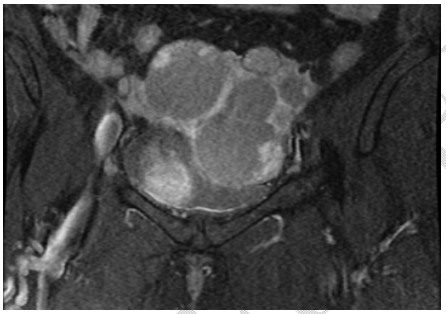

(f) Coronal post contrast fat suppressed T1WI

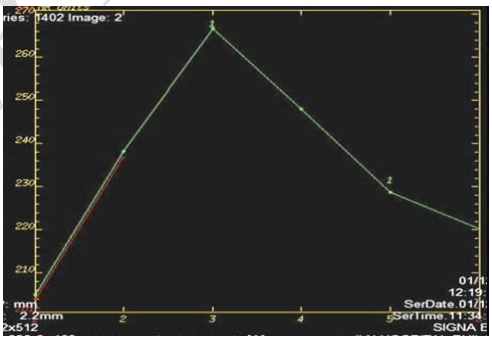

(e) Post processing time intensity curve

Figure 3 :shows bilateral large ovarian complex cystic lesions, measuring about 9x5cm on the right side and 10x6cm on the left side, displaying low signals on T1WIs (a), heterogeneous signals on T2WIs (b), restricted diffusion (c), ADC value of ($1.1x10^{-3}mm^2/s$)(d), and type III time intensity curve(rapid enhancement with rapid wash out),suggesting their malignant nature

Discussion

The mean value of CA 125 in patients with ovarian cancer was 380.35± 400.23 U/ml which was significantly higher than that for the benign ovarian lesions (28 ± 20 U/ml (P<0.001). A finding that is comparable to a study by Yingchun and colleagues [16]which showed that

serum CA125 of serous carcinoma patients was (301.45 ±104.42) U/mL, which was significantly higher than that in patients with benign ovarian serous cystadenoma($P<0.05$).

MRI has a sensitivity of 53.85% whereas DWI had a sensitivity of 88.89%. The addition of DWI to MRI is anticipated to boost the specificity and validity of the test since the specificity for DWI was 100% versus traditional MRI's 92.59%, and the correctness was 97% compared to MRI's 80%.

The mean ADC readings for malignant tumors in the quantitative evaluation were ($1.1x10^{-3}$ ±0.42 SD mm^2/s), whereas those for benign tumors were ($1.84x10^{-3}$ ±0.8 SD mm^2/s) with a cutoff value of $1.1x10^{-3}$.

Due to the heterogeneous cellularity of the teratoma, mature teratomas exhibited limited diffusion with average ADC values of 0.9 x 10^{-3} (false positive). Because of the heterogeneous cellular composition of other tumors, such as tubo-ovarian abscesses, mucinous cystadenomas, endometriomas, and ovarian hemorrhagic cysts, diffusion was impeded in these masses (mean ADC values of 0.60, 0.80, 0.90, and 0.5 X 10^{-3}).

Based on 131 individuals with pelvic masses, Li and colleagues' [7]study (46 benign and 85 malignant). In this research, the solid component of malignant and benign ovarian surface epithelial tumors was compared in terms of their ADC values in order to preoperatively distinguish between benign and malignant ovarian tumors. Between benign and malignant lesions, there was a substantial difference in the mean ADC value assessed for the solid component. Their findings imply that a cutoff point for the ADC that best distinguishes between malignant and benign ovarian tumors may be $1.25x10^{-3}$ mm^2/s. Unlike our investigation, where a cutoff point of $1.1x10^{-3}mm^2/s$ for the ADC was used to distinguish between malignant and benign ovarian tumors. Additionally, after including DWI into the traditional MR in their investigation, the sensitivity, specificity, and accuracy were 96.5%,

89.1, and 93.1%, respectively. Sensitivity, specificity, and accuracy were 88.89%, 100%, and 97% in our research.

El Ameen and colleagues conducted a research recently [17]on 47 individuals with pelvic tumors (25 malignant, 18 benign, and 4 borderline,), with a mean age of 39 ±15.9 years old; in our study, it was 38.17 ±11.7 years. The DWI-based diagnosis in this investigation had 100% sensitivity, while the specificity was just 88%. The existence of 8 benign tumors that resembled cancer explained the poor specificity. These tumors comprised benign sclerosing tumors, mature cystic teratomas, and struma ovarii. Due to the heterogeneous cellularity of the lesions, they all had limited diffusion and average ADC values of 0.9 $\times 10^{-3}$ mm^2/s, 0.8 $\times 10^{-3}$ mm^2/s, 1 $\times 10^{-3}$ mm^2/s, respectively, showing (false positive instances). The average ADC readings for benign lesions were 1.7 ±0.6 $\times 10^{-3} mm^2/s$, (this was similar to our research where it was 1.84 ±0.8 $\times 10^{-3} mm^2/s$), whereas those for borderline and malignant lesions were 0.9 ±0.2 $\times 10^{-3} mm^2/s$ and 0.8 ±0.1, respectively. According to our findings, the threshold value for ADC in cancer is $\leq 1 \times 10^{-3}$ mm^2/s.

Another study carried in 2020 by Ali and colleagues [18]as traditional MRI and DWI were done on 51 individuals with complicated cystic or solid adnexal tumors identified by gynecological ultrasonography. When the surgical and histopathologic outcomes were compared with the results, it was found that 23 of the 51 women (45%) had malignant ovarian tumors and 28 of the 51 women (55%) had benign ovarian pathologies (in our study pathology proved 65% benign cases and 35% malignant cases). The average ADC value for ovarian cancers was 0.977 ±0.32 $\times 10^{-3} mm^2/s$, which was much lower than the average ADC values for benign ovarian tumors, which were 1.516 ±0.6 $\times 10^{-3} mm^2/s$, with a cutoff value of less than 1.17 $\times 10^{-3} mm^2/s$. The combined pictures demonstrated 84.3% effectiveness, 71.4% specificity, and 100% sensitivity. However, the ovarian lesion was characterized with 80% accuracy using conventional MRI alone without DWI, with 91.3% sensitivity and 64.29%

specificity. In our investigation, the accuracy was 97%, the specificity was 100%, and the sensitivity was 88.89%.The accuracy of conventional MRI alone was 80%, the sensitivity was 53.85 % and the specificity was 92.59 %.

In our study the sensitivity of DCE-MRI was more than conventional MRI (77.15 %). The specificity was higher for DCE (100%) compared to pre-contrast MRI sequences (92.59%), otherwise, as the accuracy of both was nearly the same with slight increase regarding the DCE-MRI which was 82.5% and 80% for conventional MRI.

Early contrast uptake was more noted with malignant lesions, while most of benign tumors showed delayed uptake.

The first peak of contrast uptake for malignant lesions varied from 55 to 110 seconds, with a mean of 76 seconds, while the MRE% varied from 125 to 330%, with a mean of 220.9%. The MRE% ranged from 25 to 128% with a mean of 84.7% for benign lesions, whereas the period of peak ranged from 60 to 260 seconds with just an average of 100 seconds.

All benign lesions 26 cases (100%) showed type-I TIC, 6 malignant cases (35.7%) showed a type-III TIC, while 8 (57.2%) cases showed a type-II TIC with a statistically significant difference between malignant and benign tumors.

Li and colleagues conducted research on 102 challenging ovarian masses in 2017 [1] (malignant 71, benign 15, and borderline 16). With a substantial significant distinction between malignant and benign tumors (P <0.001), 59 of 71 (83%) malignant tumors displayed a type-III TIC, 9 of 16 (56%) borderline tumors had a type-II TIC, and 10 of 15 (67%) benign tumors displayed a type-II TIC. There was no type-I TIC in any of the malignant tumors, and no type-III TIC in any of the benign masses.

47 individuals with ovarian masses were the subjects of a research by El Ameen and colleagues [17]. (25 malignant, 18 benign, and 4 borderline). They discovered that the MRP's duration of signal intensity curves type II and III accurately predict the likelihood of

malignancy with a sensitivity and specificity of 88% and 92%, respectively. It was discovered that curve type I had a 100% specificity for benign ovarian tumors, which is consistent with our results. Only one instance with curve type III was benign; it was pathologically determined to be an ovarian benign sclerosing tumor. The increased vasculature of sclerosing stromal tumors provides an explanation for this outcome.

33 examples of heterogeneous ovarian tumors were the subject of a research conducted in 2021 by Singla and colleagues [19]. DCE-MRI, DW imaging, apparent diffusion coefficient, and T1 and T2 weighted sequences were used. 2/33 tumors were borderline, 20/33 were benign, and 11/33 were malignant. A 100% specificity for malignant tumorswas shown by the Type III curve. Type III TIC was found in only malignant lesions, whereas type I TIC was observed in only benign lesions, consistent with our findings. Eight (72.7%) of the 11 malignant cases with pathological proof had type III curves, three (27.3%) type II curves, and none had type I curves. Type I curves were seen in 14 (70%) in the benign group, type II in 6 (30%) and type III in nothing. The 8tumors exhibiting type III curve were all cancerous, whereas all 14 lesions exhibiting type I curve were benign. In line with our investigation, a significant difference between the kinds of lesions showing type I and type III curves was observed (p=0.001).

Neither of the benign lesions in our analysis had an O-RADS MRI score of 4 or 5. According to research by Cao and colleagues [20], >O-RADS 3 was the ideal cutoff point for diagnosing malignancy. The research included 1054 adnexal lesions, of which 750 were benign and 304 were malignant. With a cutoff value of >O-RADS 3, the malignancy percentages of O-RADS 5, 4, 3, and 2 lesions were 89.57%, 34.46%, 1.10%, and 0.45%, respectively.

Conclusions:

Conventional MR images are the mainstays for assessment of patients with adnexal lesions.The addition of DWI and DCE-MR imaging enhances the specificity of MRI,

boosting the radiologist's confidence in picture interpretation and ultimately affecting the patients' prognosis.

References:

1. Li HM, Qiang JW, Ma FH, Zhao SH. The value of dynamic contrast-enhanced MRI in characterizing complex ovarian tumors. J Ovarian Res. 2017;10:4.

2. Pereira PN, Sarian LO, Yoshida A, Araújo KG, Barros RHO, Baião AC, et al. Accuracy of the ADNEX MR scoring system based on a simplified MRI protocol for the assessment of adnexal masses. Diagn Interv Radiol. 2018;24:63-71.

3. Xu Y, Yang J, Zhang Z, Zhang G. MRI for discriminating metastatic ovarian tumors from primary epithelial ovarian cancers. J Ovarian Res. 2015;8:61.

4. Sohaib SA, Sahdev A, Van Trappen P, Jacobs IJ, Reznek RH. Characterization of adnexal mass lesions on MR imaging. AJR Am J Roentgenol. 2003;180:1297-304.

5. Whittaker CS, Coady A, Culver L, Rustin G, Padwick M, Padhani AR. Diffusion-weighted MR imaging of female pelvic tumors: a pictorial review. Radiographics. 2009;29:759-74; discussion 74-8.

6. Lam CZ, Chavhan GB. Magnetic resonance imaging of pediatric adnexal masses and mimics. Pediatr Radiol. 2018;48:1291-306.

7. Li W, Chu C, Cui Y, Zhang P, Zhu M. Diffusion-weighted MRI: a useful technique to discriminate benign versus malignant ovarian surface epithelial tumors with solid and cystic components. Abdom Imaging. 2012;37:897-903.

8. Priest AN, Gill AB, Kataoka M, McLean MA, Joubert I, Graves MJ, et al. Dynamic contrast-enhanced MRI in ovarian cancer: Initial experience at 3 tesla in primary and metastatic disease. Magn Reson Med. 2010;63:1044-9.

9. Young RH, Scully RE. Sex cord-stromal, steroid cell, and other ovarian tumors with endocrine, paraendocrine, and paraneoplastic manifestations. Blaustein's Pathology of the female Genital Tract2002. p. 905-66.

10. Mohaghegh P, Rockall AG. Imaging strategy for early ovarian cancer: characterization of adnexal masses with conventional and advanced imaging techniques. Radiographics. 2012;32:1751-73.

11. Kyriazi S, Kaye SB, deSouza NM. Imaging ovarian cancer and peritoneal metastases--current and emerging techniques. Nat Rev Clin Oncol. 2010;7:381-93.

12. Thoeny HC, De Keyzer F. Extracranial applications of diffusion-weighted magnetic resonance imaging. Eur Radiol. 2007;17:1385-93.

13. Mansour S, Wessam R, Raafat M. Diffusion-weighted magnetic resonance imaging in the assessment of ovarian masses with suspicious features: Strengths and challenges. Egypt J Radiol Nucl Med. 2015;46:1279-89.

14. Thomassin-Naggara I, Bazot M, Daraï E, Callard P, Thomassin J, Cuenod CA. Epithelial ovarian tumors: value of dynamic contrast-enhanced MR imaging and correlation with tumor angiogenesis. Radiology. 2008;248:148-59.

15. Kishimoto K, Ito K, Awaya H, Matsunaga N, Outwater EK, Siegelman ES. Paraovarian cyst: MR imaging features. Abdom Imaging. 2002;27:685-9.

16. Yingchun D, Lingling B, Xiaopeng Y. Study of Abdominal Color Doppler Ultrasound Combined with CA125 in the Diagnosis of Ovarian Serous Tumors. IMAGING SCIENCE AND PHOTOCHEMISTRY. 2022;40:133-7.

17. El Ameen NF, Eissawy MG, Mohsen LAMS, Nada OM, Beshreda GM. MR diffusion versus MR perfusion in patients with ovarian tumors; how far could we get? Egypt J Radiol Nucl Med. 2020;51:35.

18. Ali RF, Nassef HH, Ibrahim AM, Chalabi NAM, Mohamed AM. The Role of Diffusion Weighted Imaging in suspected cases of ovarian cancer. Egypt J Radiol Nucl Med. 2020;51:97.

19. Singla V, Dawadi K, Singh T, Prabhakar N, Srinivasan R, Suri V, et al. Multiparametric MRI Evaluation of Complex Ovarian Masses. Curr Probl Diagn Radiol. 2021;50:34-40.

20. Cao L, Wei M, Liu Y, Fu J, Zhang H, Huang J, et al. Validation of American College of Radiology Ovarian-Adnexal Reporting and Data System Ultrasound (O-RADS US): Analysis on 1054 adnexal masses. Gynecol Oncol. 2021;162:107-12.